Dinuclear copper(II) and copper(I) complexes of tetradentate (N_4) thio-diazine ligands; synthetic, structural, magnetic and electrochemical studies. *In situ* oxidation of copper(I) complexes to produce dinuclear hydroxo-bridged copper(II) complexes

Liqin Chen, Laurence K. Thompson* and John N. Bridson

Department of Chemistry, Memorial University of Newfoundland, St John's, Nfld, A1B 3X7 (Canada)

(Received March 24, 1993, revised June 22, 1993)

Abstract

Hydroxo-bridged dinuclear copper(II) complexes of the tetradentate diazine ligand PTPH (1,4-di-(2'-pyridylthio)-phthalazine) [$(Cu_2(PTPH)(OH)X_3)$ (X = Cl (**I**), Br (**II**)) were synthesized by the aerial oxidation of copper(I) complexes, prepared *in situ*. A dinuclear copper(I) perchlorate complex of PTPH $[Cu_2(PTPH)_2](ClO_4)_2 \cdot 2CH_3CN$ (**III**) was also isolated, which involved two adjacent tetrahedral copper(I) centers bound between two tetradentate ligands. **I** crystallizes in the monoclinic system, space group $P2_1/n$, with $a = 11.065(2)$, $b = 12.907(6)$, $c = 20.053(2)$ Å, $\beta = 90.59(1)°$, and four formula units per unit cell. **III** crystallizes in the triclinic system, space group $P\bar{1}$, with $a = 11.220(4)$, $b = 11.397(3)$, $c = 10.561(3)$ Å, $\alpha = 92.92(2)$, $\beta = 115.32(2)$, $\gamma = 108.22(2)°$ and two formula units per unit cell. Attempts to synthesize hydroxo-bridged complexes in aqueous medium were unsuccessful, and in basic medium resulted in the decomposition of the ligand. This was confirmed by the preliminary X-ray structure of the product of the reaction of PTPH with $CuCl_2$ in $MeOH/NEt_3$, which indicated the ligand fragment to be 1-methoxy-4-(2'-pyridylthio)phthalazine (PTPO) in a unique structural arrangement involving three different mononuclear copper(II) centers in $[Cu(PTPO)_2(H_2O)][CuCl_4][Cu(PTPO)Cl_2] \cdot 2.8H_2O$ (**IV**). **IV** crystallizes in the monoclinic system, space group $P2_1/c$, with $a = 15.386(6)$, $b = 25.248(7)$, $c = 13.95(2)$ Å, $\beta = 110.71(5)°$ and four formula units per unit cell. The dinuclear copper(II) complexes have low room temperature magnetic moments and variable temperature magnetic measurements show moderately strong antiferromagnetic coupling ($-2J > 360$ cm^{-1}). Compounds **I** and **II** exhibit two-electron reduction steps at positive potentials 0.41–0.43 V (versus SCE) to produce rearranged dinuclear copper(I) species.

Introduction

In previous papers we have reported a series of studies on dinuclear and tetranuclear complexes of the tetradentate, N_4, diazine ligands 1,4-di-(2'-pyridylthio)phthalazine (PTPH) and 3,6-di-(2'-pyridylthio)pyridazine (PTP) [1–6] (Fig. 1). These two ligands usually form halogen-bridged dinuclear copper(II) complexes when they are reacted directly with copper(II) halides, even in solvents containing appreciable amounts of water [6], and the direct synthesis of hydroxy-bridged species, so common with the pyridylaminophthalazine (PAPR = 1,4-di-(2'-pyridyl(R)amino)phthalazine) ligands ($[Cu_2(PAPR)(OH)X_3]$ (X = Cl, Br, IO_3, NO_3, SO_4, etc.)) in water [7], has been unsuccessful, despite an earlier report to the contrary [2]. In the case of PTP the use of triethylamine was necessary to produce the complexes $[Cu_2(PTP)(OH)X_3]$ (X = Cl, Br) [5], and although these compounds have not been structurally confirmed, their magnetic and spectral properties clearly indicate them to be hydroxy-bridged derivatives [5]. The case for PTPH is different, and reaction with copper(II) halides in methanol/H_2O/NEt_3 does not pro-

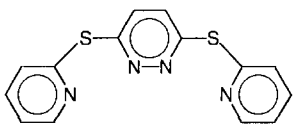

PTP

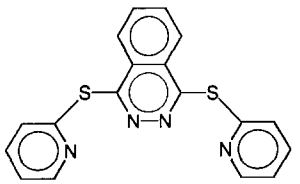

PTPH

Fig. 1. Structures of PTPH and PTP

*Author to whom correspondence should be addressed.

0020-1693/93/$6.00

duce hydroxy-bridged species, but instead ligand decomposition occurs. It is interesting to note that hydroxy-bridged copper(II) nitrate complexes of PTPH and PTP were, however, synthesized directly in $MeOH/H_2O$ or $CHCl_3/CH_3CN$ mixtures [2, 6].

In this report we describe the synthesis of hydroxo-bridged dinuclear copper(II) halide complexes of PTPH by an unusual synthetic procedure, in which the copper(I) complexes are oxidized *in situ* by reaction with air. The variable temperature magnetic properties and electrochemical properties of these systems will be discussed and compared with relevant compounds, which are structurally similar. Variable temperature magnetism has also been carried out on $[Cu_2(PTP)(OH)(NO_3)_3]$ (**V**) [2], which has been previously reported.

Experimental

Physical measurements

C, H and N analyses were carried out by the Canadian Microanalytical Service, Delta, Canada. Room temperature magnetic moments were measured by the Faraday method using a Cahn 7600 Faraday magnetic susceptibility system. Variable temperature magnetic susceptibility data were obtained in the range 4–300 K by using an Oxford Instruments superconducting Faraday magnetic susceptibility system with a Sartorius 4432 microbalance. A main solenoid field of 1.5 T and a gradient field of 10 Tm^{-1} were employed.

IR spectra were recorded using a Mattson Polaris FTIR spectrometer and electronic spectra with a Cary 5E instrument. Electrochemical measurements were made with a BAS CV-27 voltammograph and a Hewlett-Packard X-Y recorder. The electrochemical cell consisted of a Pt wire auxiliary electrode, an SCE reference electrode and a glassy-carbon disk working electrode. All measurements were carried out in DMF (0.1 M TEAP) under a nitrogen atmosphere with 1 mM complex concentrations.

Synthesis of complexes

$[Cu_2(PTPH)(OH)Cl_3]\cdot 1.2CHCl_3$ (I) and
$[Cu_2(PTPH)(OH)Br_3]\cdot CHCl_3\cdot H_2O$ (II)

Copper powder (0.19 g, 3.0 mmol) was added to a solution of $CuCl_2\cdot 2H_2O$ (0.171 g, 1.0 mmol) in CH_3CN (20 ml), the mixture stirred under a nitrogen atmosphere until the solution became colorless, and then it was filtered into a solution of PTPH (0.175 g, 0.50 mmol) in $CHCl_3$ (20 ml) under a nitrogen atmosphere. The resulting dark red solution was allowed to stand at room temperature exposed to air for several weeks. The color of the solution changed gradually from red to brown and then to green. After leaving the green solution for a few days, dark green crystals formed which were filtered off, washed with CH_3CN and $CHCl_3$ and air dried. Yield 0.105 g. The crystals lost solvent slowly in air. A crystalline sample was kept under the mother liquor for subsequent low temperature structural analysis. *Anal.* Calc. for $Cu_2S_2N_4OC_{18}H_{13}Cl_3\cdot 1.2CHCl_3$: C, 31.07; H, 1 93; N, 7.55. Found: C, 31.04; H, 2.04; N, 7.63%. This sample lost some chloroform on exposure to air prior to analysis. **II** was prepared in a similar manner, but the copper(I) solution took much longer to oxidize. *Anal.* Calc. for $Cu_2S_2N_4O_2C_{19}H_{16}Cl_3Br_3$: C, 26.24; H, 1.85; N, 6.44. Found: C, 26.07; H, 1.66; N, 6.26%.

$[Cu_2(PTPH)_2](ClO4)_2\cdot 2CH_3CN$ (III)

Copper powder (0.19 g, 3.0 mmol) was added to a solution of $Cu(ClO_4)_2\cdot 6H_2O$ (0.15 g, 0.4 mmol) in CH_3CN (40 ml). The mixture was stirred under a nitrogen atmosphere until the solution became colorless, and then it was filtered into a solution of PTPH (0.175 g, 0.50 mmol) in $CHCl_3$ (10 ml) under a nitrogen atmosphere. The resulting deep red solution was allowed to stand at room temperature for several days. Red crystals formed, which were filtered off, washed with CH_3CN and $CHCl_3$ and air dried. Yield 0.145 g. *Anal.* Calc. for $Cu_2S_4N_{10}O_8C_{40}H_{30}Cl_2$: C, 43.48; H, 2.74; N, 12.68. Found: C, 43.27; H, 2.55; N, 12.40%.

$\{[Cu(PTPO)_2(H_2O)][CuCl_4][Cu(PTPO)Cl_2]\}$ (IV)

PTPH (0.175 g, 0.50 mmol) was dissolved in hot methanol (40 ml) and triethylamine (1.26 g, 1.25 mmol) was added. This solution was added to a solution of $CuCl_2\cdot 2H_2O$ (0.213 g, 1.25 mmol) in H_2O (10 ml). The green solution was refluxed for 30 min and then filtered to remove some brown insoluble material. The yellowish green filtrate was left at room temperature for several days and a deep green crystalline product formed, which was filtered off, washed with ethanol and air dried. Yield 0.12 g. Crystals suitable for X-ray determination were obtained by diffusion of ethyl ether into a CH_3OH/H_2O (4:1) solution of **IV**.

$[Cu_2(PTP)(OH)(NO_3)_3]$ (V)

PTP (0.15 g, 0.5 mmol) was dissolved in $CHCl_3$ (10 ml) and a solution of $Cu(NO_3)_2\cdot 3H_2O$ (0.24 g, 1.0 mmol) in CH_3CN (30 ml) added. The resulting deep blue colored solution was kept at room temperature overnight, whereupon deep blue crystals formed, which were filtered off, washed with CH_3CN and air dried. Yield 0.165 g. *Anal.* Calc. for $Cu_2S_2N_7O_{10}C_{14}H_{11}$: C, 26.76; H, 1.77; N, 15.60. Found: C, 26.83; H, 1.80; N, 15.64%. This compound has been prepared previously, but by a different route [2].

Crystallographic data collection and refinement of the structures

$[Cu_2(PTPH)(OH)Cl_3]\cdot 1.5CHCl_3$ (I)

The diffraction intensities of a green irregular crystal of **I** of approximate dimensions $0.300\times0.300\times0.300$ mm were collected using a Rigaku AFC6S diffractometer with graphite monochromatized Mo Kα radiation. Cell constants and the orientation matrix were obtained by least-squares refinements of the setting angles of 16 carefully centered reflections in the range $44.63<2\theta<49.18°$. Based on a statistical analysis of the intensity distribution, and the successful solution and refinement of the structure, the space group was determined to be $P2_1/n$ (No. 14). Machine and data collection parameters and crystal data are given in Table 1. The data were collected at $-80(1)$ °C using an ω–2θ scan technique to a maximum 2θ value of 50.0°. Omega scans of several intense reflections, made prior to data collection, had an average width at half-height of 0.32° with a take-off angle of 6.0°. Scans of $(1.30+0.30\tan\theta)°$ were made at a speed of 8.0°/min (in ω). The weak reflections ($I<10.0\sigma(I)$) were re-scanned (maximum of two rescans) and the counts were accumulated to assure good counting statistics. The ratio of peak counting time to background counting time was 2:1. A total of 5583 reflections was collected. The intensities of three representative reflections, which were measured after every 150 reflections, remained constant throughout data collection (no decay correction applied). An empirical absorption correction was applied, using the program DIFABS [8], which resulted in transmission factors ranging from 0.81 to 1.00. The data were corrected for Lorentz and polarization effects.

The structure was solved by direct methods [8–11]. The non-hydrogen atoms were refined anisotropically. The final cycle of full-matrix least-squares refinement was based on 3869 observed reflections ($I>3.00\sigma(I)$) and 344 variable parameters and converged with unweighted and weighted agreement factor of $R=\Sigma\|F_o|-|F_c\|/\Sigma|F_o|=0.052$ and $R_w=[(\Sigma w(|F_o|-|F_c|)^2/\Sigma wF_o^2)]^{1/2}=0.054$. The standard deviation of an observation of unit weight was 2.96. The weighting scheme was based on counting statistics and included a factor ($\rho=0.01$) to downweight the intense reflections. Plots of $\Sigma w(|F_o|-|F_c|)^2$ versus $|F_o|$, reflection order in data collection, $\sin\theta/\lambda$, and various classes of indices showed no unusual trends. The maximum and minimum peaks on the final difference Fourier map corresponded to 1.11 and -1.15 electrons/Å^3, respectively, and have no chemical significance. Neutral atom scattering factors [11] and anomalous dispersion terms [12, 13] were taken from the usual sources. All calculations were performed using the TEXSAN [14] crystallographic software package using a VAX 3100 workstation. The hydrogens, except the hydroxy hydrogen, were placed in calculated positions with their thermal parameters set to 20%

TABLE 1. Summary of crystal, intensity collection and structure refinement data for **I** and **III**

	I	III
Formula	$Cu_2S_2N_4OC_{19.5}H_{14.5}Cl_{7.5}$	$CuClO_4S_2N_5C_{20}H_{15}$
Crystal color	dark green	deep red
Formula weight	777.98	552.49
Crystal system	monoclinic	triclinic
Space group	$P2_1/n$	$P\bar{1}$
a (Å)	11.065(2)	11.220(4)
b (Å)	12.907(6)	11.397(3)
c (Å)	20.053(2)	10.561(3)
α (°)	90.0	92.92(2)
β (°)	90.59(1)	115.32(2)
γ (°)	90.0	108.22(2)
V (Å^3)	2864(1)	1132 4(7)
D_{calc} (g cm^{-3})	1 804	1.620
Z	4	2
Absorption coefficient μ (cm^{-1})	23.60	12.98
Radiation, λ (Å)	Mo Kα, 0.71069	Mo Kα, 0.71069
T (°C)	-80	25
$F(000)$	1540	560
Scan rate (° min^{-1})	8 0	16.0
$2\theta_{max}$ (°)	50.0	52.1
Data collected	5583	4703
No unique data	3869 ($I>3\sigma(I)$)	2707 ($I>3\sigma(I)$)
No variables	344	299
GOF	2.96	2.24
R	0 052	0 046
R_w	0 054	0 043

higher than their bonded partners. The hydroxy hydrogen was found in a difference map. Two chloroform solvent molecules were found, one disordered at a special position. The atomic coordinates are given in Table 2. For hydrogen atom coordinates (Table S1), and thermal parameters (Table S2), see 'Supplementary material'.

III and IV

The same procedures were used for these compounds. Crystal and other data for **III** are listed in Table 1, and atomic coordinates are listed in Table 3. For hydrogen atom coordinates (Table S3) and thermal parameters (Tables S4), see 'Supplementary material'. Full structural details for **IV** are not reported because of the presence of non-stoichiometric solvent in the lattice, and the fact that the sample decomposed in the X-ray beam. Current refinement ($R=0.109$, $R_w=0.093$) has, however, established the presence of the three copper containing fragments and the gross structure.

TABLE 2. Final atomic positional parameters and B_{eq} values for $[Cu_2(PTPH)(OH)Cl_3]$ 1.5$CHCl_3$ (**I**)

Atom	*x*	*y*	*z*	B_{eq}
Cu(1)	0.84225(7)	0.13858(6)	0.91789(4)	1 53(3)
Cu(2)	0.84202(7)	0.15407(6)	1.06813(4)	1 57(4)
Cl(1)	0.6956(2)	0.0624(1)	0.85689(9)	2.39(8)
Cl(2)	0.7462(1)	0.2918(1)	0 98616(9)	2.00(7)
Cl(3)	0.7032(2)	0 0834(1)	1 1360(1)	2.50(8)
Cl(4)	0.4817(3)	0 3841(3)	0 8210(2)	8.0(2)
Cl(5)	0 4059(5)	0 5045(5)	0.9308(2)	21.7(5)
Cl(6)	0.6135(7)	0.5603(4)	0 8585(4)	20.1(5)
Cl(7)	0 406(1)	−0 0752(6)	0.538(1)	15(1)
Cl(8)	0 5988(7)	0.0564(7)	0 5540(7)	8 3(5)
Cl(9)	0.511(2)	0.023(2)	0 4260(4)	18(1)
S(1)	1.1047(2)	0 1280(2)	0 83989(9)	2.39(8)
S(2)	1.1078(2)	0 1700(2)	1 1488(1)	2 9(1)
O(1)	0 8132(3)	0.0586(3)	0 9966(2)	1 5(2)
N(1)	0 8913(5)	0.2314(4)	0.8434(3)	1 8(3)
N(2)	1 0119(4)	0.1553(4)	0.9594(3)	1 4(2)
N(3)	1 0114(4)	0.1650(4)	1 0273(3)	1 6(2)
N(4)	0 8879(5)	0.2625(5)	1.1354(3)	2.1(3)
C(1)	0 8148(6)	0 3044(6)	0 8214(4)	2.2(3)
C(2)	0 8386(6)	0 3686(6)	0.7684(4)	2 5(3)
C(3)	0 9470(7)	0 3573(6)	0.7357(3)	2 7(4)
C(4)	1.0309(6)	0.2861(6)	0.7593(3)	2 4(3)
C(5)	0.9986(6)	0 2249(6)	0.8130(3)	2.0(3)
C(6)	1.1130(6)	0 1546(5)	0 9270(3)	1.6(3)
C(7)	1.2297(5)	0 1684(5)	0.9594(3)	1.6(3)
C(8)	1 3401(6)	0 1687(5)	0 9240(4)	2.3(3)
C(9)	1 4450(6)	0 1799(6)	0 9599(4)	3 1(4)
C(10)	1.4460(6)	0.1899(6)	1.0289(4)	2 9(4)
C(11)	1.3396(6)	0.1906(6)	1.0636(4)	2 4(3)
C(12)	1 2284(5)	0.1783(5)	1.0288(3)	1 5(3)
C(13)	1 1144(6)	0 1736(5)	1 0608(3)	1 9(3)
C(14)	0 9943(6)	0.2621(6)	1 1683(3)	2 1(3)
C(15)	1.0185(7)	0.3296(6)	1.2210(4)	3 0(4)
C(16)	0.9276(8)	0.3978(6)	1 2401(4)	3 5(4)
C(17)	0.8202(7)	0.4002(6)	1 2052(4)	3.0(4)
C(18)	0 8034(6)	0 3314(6)	1 1533(4)	2 6(3)
C(19)	0 531(1)	0 460(1)	0.8874(6)	9 3(9)
C(20)	0.471(2)	0 025(2)	0.505(1)	6(1)

$B_{eq}=(8\pi^2/3)\Sigma_{i=1}^{3}\Sigma_{j=1}^{3}U_{ij}a^*_i a^*_j \vec{a}_i \vec{a}_j$.

TABLE 3 Final atomic positional parameters and B_{eq} values for $[Cu_2(PTPH)_2]\cdot(ClO_4)_2$ 2CH_3CN (**III**)

Atom	*x*	*y*	*z*	B_{eq}
Cu(1)	0.52408(8)	−0.02520(7)	0 35834(8)	3 17(3)
Cl(1)	0.0457(2)	0.3217(2)	0.7464(2)	4 78(7)
S(1)	0.3284(2)	0.0333(1)	0 0723(2)	3.46(5)
S(2)	0.2338(2)	0.1234(2)	0 6044(2)	3.82(6)
O(1)	0 0564(5)	0.3593(4)	0 6250(5)	6.2(2)
O(2)	0 1784(5)	0 3334(5)	0.8553(5)	6.8(2)
O(3)	−0.0496(6)	0 1988(5)	0 7091(6)	11.7(3)
O(4)	0.0014(7)	0 4037(7)	0 8022(7)	10.9(3)
N(1)	0.5990(5)	0 1218(4)	0.2781(5)	2.9(2)
N(2)	0.3528(4)	0 0173(4)	0 3297(4)	2.5(1)
N(3)	0.3331(4)	0 0373(4)	0.4494(5)	2.5(1)
N(4)	0 5186(5)	0.2033(4)	0 7338(5)	3 1(2)
N(5)	0.4886(7)	0.3300(6)	0 4228(7)	6 5(3)
C(1)	0 7312(6)	0.2094(6)	0 3487(6)	3 5(2)
C(2)	0 7737(7)	0.3191(6)	0 3037(7)	4 0(2)
C(3)	0 6803(8)	0.3422(6)	0 1832(7)	4 2(2)
C(4)	0 5447(7)	0.2552(6)	0 1101(6)	3 7(2)
C(5)	0 5076(6)	0.1473(5)	0 1623(6)	2.8(2)
C(6)	0 2828(5)	0 0527(5)	0 2119(5)	2 5(2)
C(7)	0.1807(5)	0 1081(5)	0 1963(6)	2 6(2)
C(8)	0.1105(6)	0 1522(5)	0 0738(6)	3.2(2)
C(9)	0.0153(6)	0 2042(6)	0 0675(6)	4 0(2)
C(10)	−0 0161(6)	0 2134(6)	0 1815(7)	4 6(3)
C(11)	0.0536(6)	0.1745(6)	0.3047(7)	3 8(2)
C(12)	0 1546(5)	0 1225(5)	0 3154(6)	2.7(2)
C(13)	0 2410(5)	0 0894(5)	0 4411(6)	2.5(2)
C(14)	0.4104(6)	0 2418(5)	0.7061(5)	3.0(2)
C(15)	0.4268(7)	0 3627(6)	0.7544(6)	4.1(2)
C(16)	0.5650(9)	0 4517(6)	0.8335(7)	5.0(3)
C(17)	0.6764(7)	0 4148(6)	0 8602(6)	4.6(2)
C(18)	0.6493(7)	0 2911(6)	0 8084(6)	3.8(2)
C(19)	0 5977(8)	0.4050(6)	0 4846(7)	4 3(3)
C(20)	0 7386(8)	0 5053(7)	0 5666(7)	6 0(3)

$B_{eq}=(8\pi^2/3)\Sigma_{i=1}^{3}\Sigma_{j=1}^{3}U_{ij}a^*_i a^*_j \vec{a}_i \vec{a}_j$

Results and discussion

X-ray crystal structures of complexes I, III and IV

A perspective view of **I** is shown in Fig. 2, and selected bond distances and angles relevant to the copper coordination spheres are given in Table 4. The two square-pyramidal copper(II) centers are bound in a triple bridged arrangement involving an axial chloro bridge, and equatorial hydroxo and phthalazine bridges. The angle at the hydroxo bridge is 104.0(2)°, the angle at the chlorine bridge is 69.87(5)°, and the copper–copper separation is 3.019(1) Å. The two equatorial copper–chlorine bonds are relatively short (Cu(1)–Cl(1)

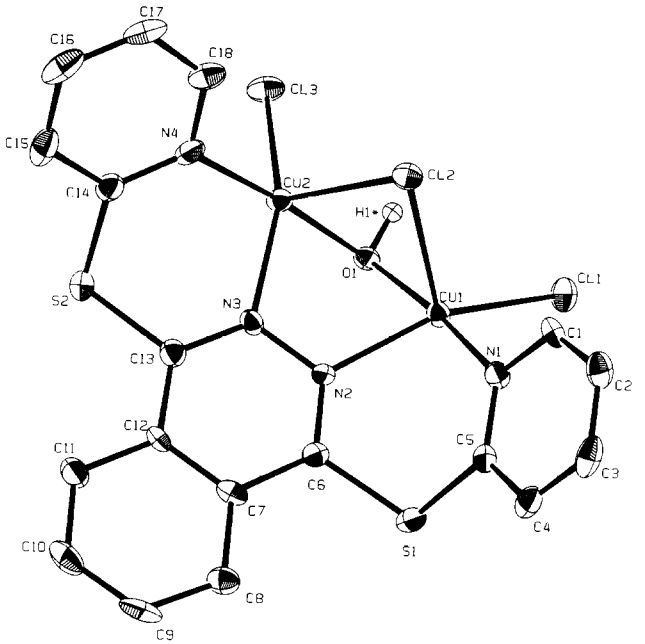

Fig. 2. Structural representation of $[Cu(PTPH)(OH)Cl_3]$ $1.5CHCl_3$ (**I**) with hydrogen atoms omitted (40% probability thermal ellipsoids).

TABLE 4. Interatomic distances (Å) and angles (°) relevant to the copper coordination spheres in $[Cu_2(PTPH)(OH)Cl_3]$ $1.5CHCl_3$ (**I**)

Cu(1)–Cl(1)	2 248(2)	Cl(1)–Cu(1)–O(1)	95.0(1)
Cu(1)–O(1)	1.915(4)	Cl(1)–Cu(1)–N(1)	93.2(2)
Cu(1)–N(1)	1 994(5)	Cl(1)–Cu(1)–N(2)	156.4(2)
Cu(1)–N(2)	2 057(5)	O(1)–Cu(1)–N(1)	171.8(2)
Cu(2)–Cl(3)	2.256(2)	O(1)–Cu(1)–N(2)	83.3(2)
Cu(2)–O(1)	1 916(4)	N(1)–Cu(1)–N(2)	89.2(2)
Cu(2)–N(3)	2 059(5)	Cl(3)–Cu(2)–O(1)	94.7(1)
Cu(2)–N(4)	2 006(6)	Cu(1)–O(1)–Cu(2)	104 0(2)
Cu(1)–Cl(2)	2 636(2)	Cl(3)–Cu(2)–N(3)	153.7(2)
Cu(1)–Cu(2)	3.019(1)	Cl(3)–Cu(2)–N(4)	92 6(2)
Cu(2)–Cl(2)	2.637(2)	O(1)–Cu(2)–N(3)	83.7(2)
O(1)–H(1)*	0 874	O(1)–Cu(2)–N(4)	172 6(2)
		N(3)–Cu(2)–N(4)	89 7(2)
		Cu(1)–Cl(2)–Cu(2)	69.87(5)
		Cu(1)–O(1)–H(1)*	110.0(2)
		Cu(2)–O(1)–H(1)*	97 0(2)

2.248(2), Cu(2)–Cl(3) 2.256(2) Å), but the apical chlorine distances are quite long (Cu(1)–Cl(2) 2.636(2), Cu(2)–Cl(2) 2.637(2) Å). The copper atoms are displaced slightly from the basal N_2ClO mean planes which can be considered to define the basal planes of the copper square-pyramids (Cu(1) 0.250(4) Å, Cu(2) 0.282(4) Å) towards Cl(2), with a dihedral angle of 45.6° between the mean basal planes. Structurally **I** resembles the analogous complex $[Cu_2(PAP)(OH)Cl_3]\cdot 1.5H_2O$ [15] (PAP = 1,4-di-(2′-pyridylamino)phthalazine), which involves two almost identical copper square-pyramids bridged in the same fashion. The Cu–Cu separation in **I** is slightly longer, and the Cu–OH–Cu angle slightly larger (average 100.9° in PAP complex). The 'bite' of each ligand is clearly comparable, and the slight differences in dinuclear center dimensions can, no doubt, be attributed to the longer C–S bonds in PTPH, compared with the C–N bonds in PAP. A unique feature of **I**, rarely seen in systems of this sort, is the hydroxide proton, located in a difference map. The angles subtended by the two coppers and the hydrogen atom at O(1) are closer to the tetrahedral angle than 120°, associated with a trigonal planar oxygen, and the solid angle (312°) implies little rehybridization, typical of so many alkoxy- and phenoxy-bridged dinuclear copper(II) complexes.

The structure of **III** is shown in Fig. 3, and interatomic distances and angles relevant to the copper coordination spheres are given in Table 5. The dinuclear cation consists of two pseudo-tetrahedral copper(I) centers, separated by 3.313(2) Å and bridged by two phthalazine groups, and forming an almost planar Cu_2N_4 hexagonal heterocyclic ring. Each ligand is bent in a 'lobster-like' *cis* conformation with both pyridine rings oriented on

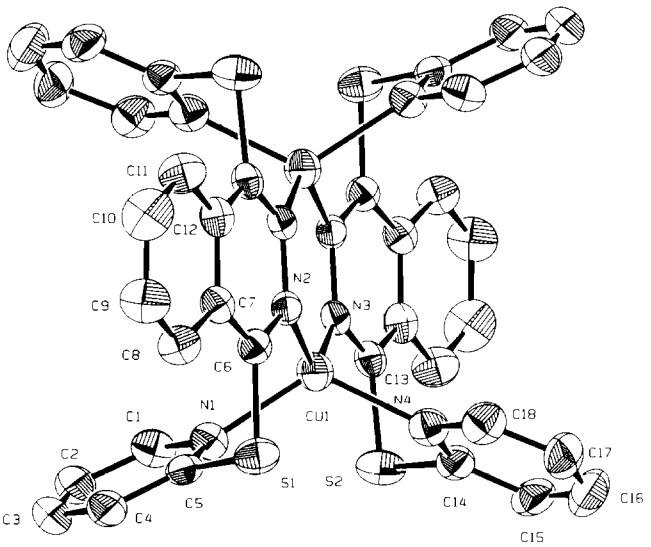

Fig. 3. Structural representation of $[Cu_2(PTPH)_2]$ $(ClO_4)_2\cdot 2CH_3CN$ (**III**) with hydrogen atoms omitted (40% probability thermal ellipsoids)

TABLE 5. Interatomic distances (Å) and angles (°) relevant to the copper coordination spheres in $[Cu_2(PTPH)_2](ClO_4)_2$ $2CH_3CN$ (**III**)

Cu(1)–N(1)	2.026(4)	N(1)–Cu(1)–N(2)	92.9(2)
Cu(1)–N(2)	2.030(4)	N(1)–Cu(1)–N(3)	115.1(2)
Cu(1)–N(3)	2.023(4)	N(1)–Cu(1)–N(4)	119.6(2)
Cu(1)–N(4)	2 022(5)	N(2)–Cu(1)–N(3)	123 4(2)
Cu(1)–Cu(1)′	3.313(2)	N(2)–Cu(1)–N(4)	115.8(2)
		N(3)–Cu(1)–N(4)	92.5(2)

the same side of the phthalazine group. Within each ligand the pyridine rings have dihedral angles of 124.4° relative to the mean phthalazine plane. The overall structure is very similar to that of $[Cu_2(PTP)_2](ClO_4)_2$ [3], which has a slightly longer Cu–Cu separation (3.422(1) Å). The copper–nitrogen separations (2.022–2.030 Å) are slightly longer than those in $[Cu_2(PTP)_2](ClO_4)_2$, but are quite normal. It is of interest to compare the structure of **III** with that of the complex $[Cu_4(dppn)_4](CF_3SO_3)_4$ (dppn = 3,6-bis(2′-pyridyl)-pyridazine) [16], which involves a similar N_4 diazine ligand, but which has a rather different 'bite'. Dppn forms five-membered chelate rings at each metal and two pairs of ligands bridge two pairs of metals, with a planar arrangement of four tetrahedral copper centers and two ligands lying above and below the Cu_4 plane. Inevitably the larger ligand 'bite' leads to larger copper–copper separations (3.566(1), 3.582(1) Å).

The preliminary structure of **IV** is shown in Fig. 4, which includes just the diazine ligand fragments. This complex is most unusual and includes three different mononuclear copper(II) centers. One is the familiar pseudo-tetrahedral $CuCl_4^{2-}$ anion. The other two involve the new ligand 1-methoxy-4-(2′-pyridylthio)-phthalazine (PTPO). In one case a square-pyramidal copper (Cu(2)) is bound equatorially to two bidentate N_2 ligands, via one phthalazine and the pyridine nitrogen, with an axial contact to a water molecule. Cu(1) is four-coordinate, bonded to a similar bidentate PTPO ligand and two chlorines in a distorted square-planar arrangement. The copper–ligand distances are typical for species of this sort. Although this crystal gave a good data set and solved easily, the final refinement was poor. This was attributed to the presence of non-stoichiometric water at several sites in the unit cell. The results nevertheless clearly account for the three unique copper fragments.

The basic structure of **V** was established by a preliminary X-ray study. The two copper(II) centers are bridged just by the pyridazine unit and a hydroxide, with a large Cu–(OH)–Cu bridge angle. However the poor current refinement, due to a disorder problem, prevents a detailed analysis of the structure at this time [17].

Reactions

The difficulty of synthesizing hydroxo-bridged dinuclear copper(II) halide complexes of PTP led to the use of the $NEt_3/MeOH/H_2O$ mixture, with the formation of $[Cu_2(PTP)(OH)X_3]$ (X = Cl, Br) [5]. Since similar

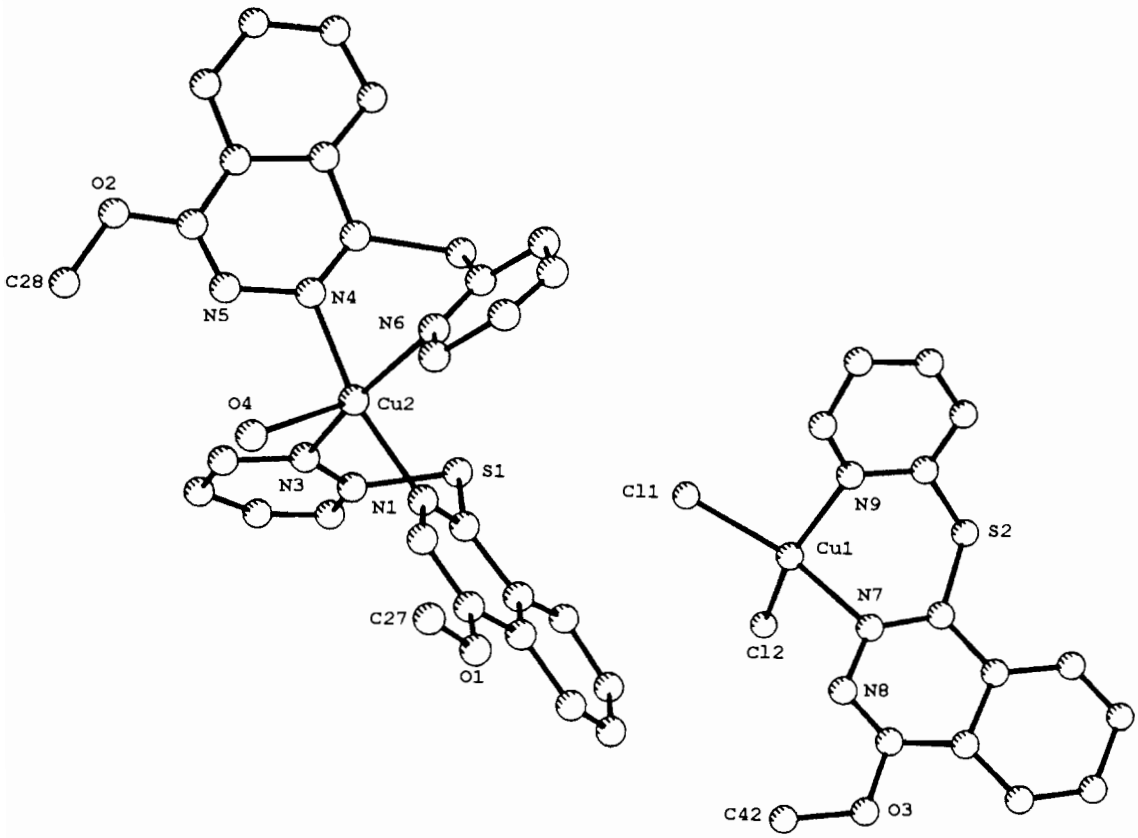

Fig. 4. Structural representation of $[Cu(PTPO)_2(H_2O)][CuCl_4][Cu(PTPO)Cl_2]$ (**IV**) showing only the two PTPO fragments

problems were encountered in the synthesis of corresponding PTPH complexes in aqueous alcoholic media, with the formation of $Cu_2(PTPH)X_4$ (X = Cl, Br) only [6], the same approach was tried with PTPH. However the expected products were not obtained and ligand decomposition occurred. The structure of **IV** reveals that a unique organic product results, and the nature of the phthalazine, PTPO, indicates that hydrolysis of PTPH has occurred. Base induced attack by methanol at a phthalazine carbon adjacent to the coordinated nitrogen could reasonably be enhanced by the electron withdrawing inductive effect of four coordinated chlorines in a dinuclear species like $Cu_2(PTPH)Cl_4$, which would clearly exist initially in the reaction mixture [6]. No pyridine thiol was detected, but in the presence of excess copper(II) salt a spontaneous redox reaction would have occurred eliminating the thiol with the formation of a copper(I) species. This presumably corresponds to the unidentified, insoluble material formed in the reaction. The question of why the same reaction does not appear to occur with PTP is pertinent, but may be largely a function of the inherent properties of the phthalazine moiety compared with the pyridazine. It is well known that 1,4-dichlorophthalazine is much more hydrolytically unstable than 3,6-dichloropyridazine, forming the corresponding mono-hydroxy species with ease.

The synthesis of the desired hydroxide-bridged complexes of PTPH was finally achieved by the oxidation of their copper(I) analogues in air. The red solutions produced by the reaction of $[Cu(CH_3CN)_4]X$ (X = Cl, Br) in acetonitrile with PTPH can reasonably be associated with species like the air stable, red, dimeric complex $[Cu_2(PTPH)_2](ClO_4)_2$ (**III**), and in fact have identical electronic spectra. The irreversible oxidation of copper(I) complexes by oxygen to give hydroxo or alkoxo complexes is common [18, 19], but the mechanisms of such reactions are not well understood. It is presumed that they proceed through the initial formation of a dioxygen–copper complex, Cu_2–O_2, which then undergoes further reduction or reaction to give oxo and/or hydroxy products derived from fully four-electron-reduced O_2 [20–22]. We have carried out low temperature oxygenations of the dicopper(I) complexes $[Cu_2(L)_2](ClO_4)_2$ (L = PTPH, PTP) in the hope of trapping the intermediate Cu_2–O_2 species. The copper(I) complexes of these two ligands seem very stable and their red color does not change even after bubbling oxygen at −78, −25 or 0 °C in methanol–dichloromethane (1:1) mixture for as long as 2 h, or even at room temperature overnight. The red copper(I) solutions prepared from Cu(I)X (X = Cl, Br) behaved similarly.

The high stability of **III** and its PTP analogue is surprising, but may reflect an inherent thermodynamic stability of the dinuclear cation or the inability of oxygen to attack the copper centers by virtue of some steric effect. Access to the copper centers from the ends of the molecule is probably impeded by the sulfur lone pairs, which project over the ends of the cation, and it would seem reasonable that significant reorganization of the dinuclear species would be required before oxidation could proceed. Electrochemical studies for **III** in DMF (GC/Pt/SCE) show an irreversible CV wave at $E_{1/2} = +0.30$ V ($\Delta E_p = 370$ mV) indicating a thermodynamically viable oxidation, but one which must involve considerable molecular reorganization. The role of halide ion is, therefore, considered to be important and it is significant that for the oxidation reaction involving copper(I) chloride, after extended exposure to air, the rate of oxidation, although still low, was higher than for bromide. Perhaps the initial step in the process involves attack by halide, splitting the dinuclear complex cation up into two mononuclear three-coordinate species, in which the copper is bound at one end of the ligand only. Reaction with excess copper(I) chloride could then produce a 1:2 dinuclear three-coordinate species, involving copper chlorine bonds, which would render the copper centers more electrophilic (an effect which would diminish in the presence of bromide) and thus more susceptible to oxidation than the original 1:1 dinuclear species. Since the ultimate product is a hydroxy-bridged species the involvement of atmospheric water in the oxidation step seems inevitable, and a two-electron oxidation of the 1:2 copper(I) species, combined with coordination of adventitious chloride would complete the process. The addition of small amounts of water does in fact speed up the oxidation process, confirming the involvement of water in the oxidation step.

Additional support for these suggestions comes from two key experiments in which compound **III** was reacted with air in acetonitrile in the presence of tetraethylammonium chloride and tetrabutylammonium bromide for an extended period. Green crystalline materials were produced, which were shown to be identical to the hydroxy-bridged complexes **I** and **II**, respectively.

The analogous PTP compounds, $Cu_2(PTP)(OH)X_3$ (X = Cl, Br) [3], can also be prepared from Cu(I) halide reactions in the presence of air in a similar manner.

Spectroscopy and magnetism

IR spectra of **I** and **II** are almost identical in the range 4000–500 cm^{-1}, indicating the likelihood of a similar dinuclear structural arrangement in **II**. The sharp absorption at 3599 (**I**) and 3584 (**II**) cm^{-1} confirms the presence of a hydroxide bridge in **II**. In the far-IR two prominent bands at 295, 275 cm^{-1} for **I** and 272, 240 cm^{-1} for **II** indicate copper(II) centers are coordinated by terminal and bridging halogens.

Electronic spectra (mull transmittance) for **I** and **II** have major visible d–d absorptions at 655 and 680 nm, respectively, consistent with square-pyramidal copper(II) centers. Complex **IV** has a more complicated Vis–near-IR spectrum with a major, broad asymmetric absorption at 680 nm and a prominent shoulder at 980 nm. The tetrahedrally distorted $CuCl_4^{2-}$ anion would be expected to exhibit d–d absorption at relatively low energy and would reasonably be associated with the 980 nm band. The broad band at 680 nm is associated with both the square-pyramidal $[Cu(PTPO)_2(H_2O)]^{2+}$ and distorted square-planar $[Cu(PTPO)Cl_2]$ species. The red copper(I) complex (**III**) has a solution (CH_3CN) spectrum dominated by two intense charge transfer bands at 277 and 322 nm, associated with the dinuclear copper(I) cation. Mixtures of PTPH and excess Cu(I)X (X = Cl, Br), produce red solutions in CH_3CN with identical spectra, indicating the presence of the same dinuclear cation in these solutions.

Room temperature magnetic moments (Table 6) for **I** and **II** are significantly lower than the spin only value for copper(II), indicating antiferromagnetic coupling between the copper centers. Variable temperature (4–300 K) magnetic data were obtained for **I**, **II** and the complex $[Cu_2(PTP)(OH)(NO_3)_3]$ (**V**). A plot of the experimental susceptibility data for **I** is given in Fig. 5. The Neél maximum in the profile is higher than 300 K indicating strong antiferromagnetic coupling between the copper centers. The rise in susceptibility at low temperatures indicates the presence of a small amount of paramagnetic impurity. The data were fitted to the Bleaney-Bowers expression (eqn. (1)) [23], using the

$$\chi_m = \frac{N\beta^2 g^2}{3k(T-\theta)}[1+1/3\ \exp(-2J/kT)]^{-1}(1-\rho) + \frac{[N\beta^2 g^2]\rho}{4kT} + N\alpha \quad (1)$$

isotropic (Heisenberg) exchange Hamiltonian ($\mathscr{H} = -2JS_1S_2$) for two interacting $S = 1/2$ centers (χ_m is expressed per mole of copper atoms, $N\alpha$ is the temperature independent paramagnetism, ρ is the fraction of monomeric impurity, and θ is a corrective term for interdimer interactions) [24, 25], using a non-linear regression procedure and the best fit line (solid line in Fig. 5) was obtained for $g = 2.15(1)$, $-2J = 390(3)$ cm^{-1}, $\rho = 0.016$, $\theta = 0.10$ K, $TIP = 63 \times 10^{-6}$ emu. Similar data treatments were performed for compounds **II** and **V**, and the results are listed in Table 6. All complexes exhibit moderately strong antiferromagnetic coupling, with very small interdimer associations. Without complete structural data for **II** and **V** little can be said about such effects, but for **I** θ is considered to be small enough to be ignored. The substantially larger $-2J$ value for **V** suggests that the hydroxide bridge angle would be larger than in **I** and **II**, in keeping with former studies [7], and with the double-bridged arrangement present in **V**.

The hydroxo-bridged complexes **I** and **II** are more strongly coupled than similar complexes of PTPH, which only have dihalogen bridges [6], and this is a clear consequence of replacing an orthogonal arrangement of halogen bridges with an equatorial hydroxide. $-2J$ values for **I** and **II** are significantly larger than those reported for analogous complexes of PTP $[Cu_2(PTP)(OH)X_3$ (X = Cl, Br) [5], which on face value contradicts an earlier observation concerning the capacitive action of a fused benzene ring in diazine complexes of this sort [5, 6]. However a detailed comparison of these systems must await a structural analysis on the PTP complexes.

An internal comparison of **I** and **II** indicates that the chloro complex is slightly more strongly coupled than the bromo complex. Previous studies have shown that in isostructural pairs of halide-bridged complexes $[Cu_2(L)X_4]$ (L = PTP, PTPH; X = Cl, Br), the chloride complexes are less strongly antiferromagnetically coupled, due to a stronger electronic inductive effect associated with the bonded chlorines [5, 6]. However the observations for **I** and **II** are consistent with data for $Cu_2(PAP)(OH)X_3$ (X = Cl, Br) [7] ($-2J(Cl) = 201$ cm^{-1}; $-2J(Br) = 190$ cm^{-1}). This may be a result of the domination of the exchange situation by the hydroxide bridge. What is surprising, however, is the fact that exchange integrals for **I** and **II** have almost doubled in comparison with the PAP complexes. Structurally these complexes are all similar, with equatorial interactions to diazine and hydroxide groups, and axial, orthogonal halides. The hydroxide bridge angle in **I** (104.0(2)°) is slightly higher than those found in the

TABLE 6 Magnetic data

Compound	μ_{eff} (BM) (r.t.)	$-2J$ (cm^{-1})	g	ρ	θ (K)	R
$[Cu_2(PTPH)(OH)Cl_3]$ 1.2$CHCl_3$ (**I**)	1.23	390(3)	2.15(1)	0.016	0.1	0.89
$[Cu_2(PTPH)(OH)Br_3]$ $CHCl_3$ H_2O (**II**)	1.22	369(4)	2.05(2)	0.013	4.0	1.20
$[Cu_2(PTP)(OH)(NO_3)_3]$ (**V**)	1.04	464(11)	2.05(4)	0.022	1.8	0.99

$R = [\Sigma(\chi_{obs} - \chi_{calc})^2/\Sigma(\chi_{obs})^2]^{1/2} \times 10^2$ $TIP \times 10^6$ emu: 63 (**I**), 60 (**II**), 63 (**V**).

TABLE 7. Electrochemical data

Compound	Scan rate (mV s^{-1})	ΔE_p (mV)	$E_{1/2}$ (V vs. SCE)
$[Cu_2(PTPH)(OH)Cl_3 \cdot 1.2CHCl_3$ (**I**)	50[a]	150	0.43
	100	170	0.43
	200	210	0 42
$[Cu_2(PTPH)(OH)Br_3] \cdot CHCl_3 \cdot H_2O$ (**II**)	100	180	0.41
$[Cu_2(PTPH)_2](ClO_4)_2 \cdot 2CH_3CN$ (**III**)	100	370	0.30

[a] 1×10^{-3} to 5×10^{-4} M complex in DMF, tetraethylammonium perchlorate, glassy-carbon working electrode, and saturated calomel reference electrode.

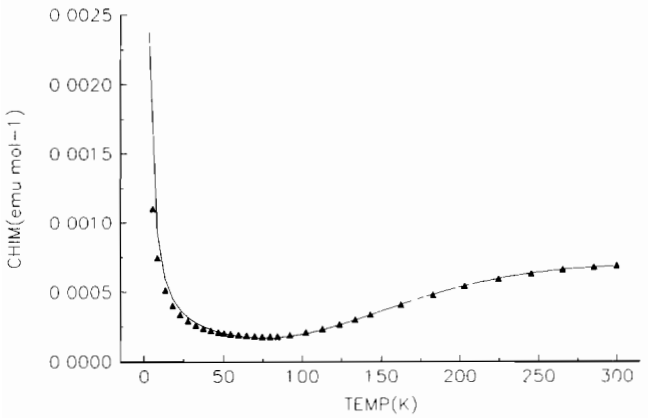

Fig 5. Magnetic data for $[Cu_2(PTPH)(OH)Cl_3]$ $1.2CHCl_3$ (**I**). The solid line was calculated from eqn. (1) with $g = 2.15(1)$, $-2J = 390(3)$ cm^{-1}, $\rho = 0\,016$, $N\alpha = 63 \times 10^{-6}$ cgsu ($R = 0.89$)

PAP complexes (100.9°(Cl); 102.1°(Br)) [15], and would only be expected to change the exchange situation by a modest amount [7]. Based on our previous analysis of the relationship between $-2J$ and the hydroxide bridge angle in a series of dinuclear copper PAP(R) complexes [7], a change in the Cu–O(H)–Cu angle of 3° would correspond to a change in $-2J$ of approx. 70 cm^{-1} and a hydroxide bridge angle of 104.0° in **I** leads to a calculated $-2J$ value which is much lower than observed ($-2J_{calc} = 255$ cm^{-1}). This suggests a fundamental difference on the part of the ligand, and in particular the role of the diazine bridge. The two ligands PAP (1,4-di-(2′-pyridylamino)phthalazine) and PTPH differ only with respect to the exocyclic groups (S in PTPH and NH in PAP). One factor can be considered that might account for the significantly different role of the phthalazine bridge in these two systems. The exocyclic NH groups could attract delocalized electron spin density within the fused diazine ring more would be the case for the less electronegative S in PTPH. This would have the effect of localizing exchange coupled spin more within the diazine ring in the PAP complexes, leading to reduced net antiferromagnetism.

Electrochemical data for **I** and **II** are listed in Table 7. Cyclic voltammetry in dried DMF showed a single redox wave for each compound with $E_{1/2}$ values in the range 0.41–0.43 V (versus SCE), associated with a sequential two-electron reduction of the dinuclear complex to a dinuclear copper(I) species. Controlled potential electrolysis in DMF at a potential of 0.1 V indicated the passage of approximately two electrons per mole. ΔE_p values vary significantly as a function of scan rate, indicating an essentially non-reversible redox process. The electrochemical behavior of **I** and **II** can be compared closely with the halogen-bridged dinuclear complexes of PTPH, $Cu_2(PTPH)X_4$ (X = Cl, Br) [6], which show much more reversible waves, associated with a two-electron reduction, at essentially the same potentials. It is reasonable to assume that on reduction significant molecular rearrangement occurs for **I** and **II**. Complex **III** exhibits a very broad wave at 0.3 V ($\Delta E_p = 370$ mV), associated with a two-electron oxidation process. The lower $E_{1/2}$ is consistent with the absence of any halide, and the very large ΔE_p value indicates a non-reversible redox process.

Supplementary material

Hydrogen atom positional parameters, thermal parameters, observed and calculated structure factors and full listings of bond distances and angles are available on request from the authors.

Acknowledgement

We thank the Natural Sciences and Engineering Research Council of Canada for financial support for this study.

References

1 S K Mandal, L.K. Thompson, M J Newlands, F.L Lee, Y Lepage, J.-P. Charland and E.J. Gabe, *Inorg. Chim Acta, 122* (1986) 199.

2 T.C. Woon, R. McDonald, S.K. Mandal, L.K Thompson, S.P. Connors and A.W. Addıson, *J Chem Soc, Dalton Trans*, (1986) 2381.
3 S.K. Mandal, L.K. Thompson, E.J Gabe, F.L. Lee and J.-P. Charland, *Inorg Chem*, *26* (1986) 2384.
4 S.K. Mandal, L.K. Thompson, E.J. Gabe, J.-P. Charland and F.L Lee, *Inorg Chem*, *27* (1988) 855
5 L.K. Thompson, S.K. Mandal, J.-P. Charland and E.J Gabe, *Can J Chem*, *66* (1988) 348.
6 L. Chen, L.K. Thompson and J.N. Brıdson, *Inorg Chem*, *32* (1993) 2938.
7 L.K. Thompson, F L. Lee and E J. Gabe, *Inorg Chem*, *27* (1988) 39.
8 N. Walker and D. Stuart, *Acta Crystallogr, Sect. A, 39* (1983) 158.
9 C.J. Gılmore, *J. Appl. Crystallogr., 17* (1984) 42.
10 P.T. Beurskens, DIRDIF, *Tech Rep 1984/1,* Crystallography Laboratory, Toernooıveld, 6525 Ed Nıjmegen, Netherlands, 1984.
11 D T. Cromer and J.T Waber, *Internatıonal Tables for X-ray Crystallography,* Vol. IV, Kynoch. Bırmıngham, UK, 1974, Table 2.2A
12 J.A Ibers and W.C. Hamilton, *Acta Crystallogr., 17* (1974) 781
13 D.T Cromer, *Internatıonal Tables for X-ray Crystallography,* Vol. IV, Kynoch, Bırmıngham, UK, 1974, Table 2 3 1.
14 *TEXSAN-TEXRAY Structured Analysıs Package,* Molecular Structure Corporatıon, The Woodlands, TX, USA, 1985
15 G. Marongıu and E.C. Lıngafelter, *Acta Crystallogr, Sect B, 38* (1982) 620
16 M -T. Youınou, N. Rahmouni, J Fıscher and J A. Osborn, *Angew. Chem, Int Ed, Engl, 31* (1992) 733.
17 L. Chen, L.K Thompson and J N. Brıdson, unpublıshed results.
18 K.D. Karlın and J Zubıeta (eds), *Bıologıcal & Inorganıc Copper Chemıstry,* Vols. 1 and 2, Adenıne, Guilderland, NY, 1986.
19 J.S. Thompson, *J Am Chem Soc, 106* (1984) 4057.
20 K.D. Karlın and Y Gultneh, *Prog Inorg Chem., 35* (1987) 219
21 K.D. Karlın, R.W. Cruse, Y Gultneh, A. Farooq, J C Hayes and J. Zubıeta, *J. Am Chem Soc, 109* (1987) 2668.
22 K.D Karlin, M.S. Haka, R W Cruse, G.J Meyer, A. Farooq, Y. Gultneh, J.C. Hayes and J. Zubıeta, *J Am Chem Soc, 110* (1988) 1196.
23 B. Bleaney and K.D Bowers, *Proc R Soc London, Ser A, 214* (1952) 451
24 K.T. McGregor, J A. Barnes and W E Hatfield, *J. Am Chem Soc, 95* (1973) 7993.
25 S. Sıkorav, I. Bkouche-Waksman and O. Kahn, *Inorg Chem*, *23* (1984) 490